APPLIED AND ENVIRONMENTAL MICROBIOLOGY, Aug. 1993, p. 2578–2588 Vol. 59, No. 8
0099-2240/93/082578-11$02.00/0

A Cytochemical Study of Extracellular Sheaths Associated with *Rigidoporus lignosus* during Wood Decay

M. NICOLE,[1]* H. CHAMBERLAND,[2] D. RIOUX,[2] N. LECOURS,[2] B. RIO,[1] J. P. GEIGER,[1] AND G. B. OUELLETTE[2]

Laboratoire de Phytopathologie, Institut Français de Recherche Scientifique pour le Développement en Coopération, B.P. 5045, 34000 Montpellier, France,[1] and Forestry Canada, Quebec Region, Sainte-Foy, Quebec G1V 4C7, Canada[2]

Received 29 January 1993/Accepted 18 May 1993

An ultrastructural and cytochemical investigation of the development of *Rigidoporus lignosus*, a white-rot fungus inoculated into wood blocks, was carried out to gain better insight into the structure and role of the extracellular sheaths produced by this fungus during wood degradation. Fungal sheaths had a dense or loose fibrillar appearance and were differentiated from the fungal cell wall early after wood inoculation. Close association between extracellular fibrils and wood cell walls was observed at both early and advanced stages of wood alteration. Fungal sheaths were often seen deep in host cell walls, sometimes enclosing residual wood fragments. Specific gold probes were used to investigate the chemical nature of *R. lignosus* sheaths. While labeling of chitin, pectin, β-1,4- and β-1,3-glucans, β-glucosides, galactosamine, mannose, sialic acid, RNA, fucose, and fimbrial proteins over fungal sheaths did not succeed, galactose residues and laccase (a fungal phenoloxidase) were found to be present. The positive reaction of sheaths with the PATAg test indicates that polysaccharides such as β-1,6-glucans are important components. Our data suggest that extracellular sheaths produced by *R. lignosus* during host cell colonization play an important role in wood degradation. Transportation of lignin-degrading enzymes by extracellular fibrils indicates that alteration of plant polymers may occur within fungal sheaths. It is also proposed that *R. lignosus* sheaths may be involved in recognition mechanisms in fungal cell-wood surface interactions.

In tropical rain forest ecosystems, soil organic compounds are rapidly degraded not only under specific conditions (e.g., high temperature and moisture levels and low oxygen concentrations) but also by active degradative systems of soil microorganisms. White-rot fungi are known to be active wood degraders since they secrete a wide range of hydrolytic and oxidative enzymes involved in plant polymer alteration (7). In tropical areas, the white-rot basidiomycete *Rigidoporus lignosus* (Klotsch) Imazeki causes severe damage to woody tissues (38) of more than 100 different species of trees. Epidemiological surveys in natural forest and rubber tree plantations in the Ivory Coast revealed a high fungal density in soil (39), suggesting that *R. lignosus* contributes actively to biodegradation of plant residues.

In the last 10 years, numerous ultrastructural investigations have contributed to a better understanding of the interface between plants and various fungi (4, 5, 14, 18, 27, 40, 50, 53, 55). There is increasing evidence that extracellular fungal sheaths (EFS), common to many fungi of different genera, are implicated in host-pathogen interactions, including attachment of hyphae to the host plant (45), cell-cell recognition (34), host penetration (35), and plant cell wall degradation (51). Extracellular coating material of both white- and brown-rotting fungi, previously characterized in vitro (30, 46, 47), were also demonstrated to be associated with wood alteration (19, 29, 37, 50). It has been suggested that early formation of slime layers might facilitate subsequent hyphal penetration of the cell wall (37, 50). EFS of *R. lignosus* were seldom described in vivo during the interaction with rubber tree roots (42, 44) but were commonly observed on wood fragments inoculated in vitro (43). There is little information on the chemical composition of EFS of wood-decaying fungi, although recent works have demonstrated the lack of chitin in the extramural substances of *R. lignosus* in infected rubber tree roots (42) and the glucan nature of sheaths of other rotting fungi (10, 50, 51).

A cytochemical study, based mainly upon colloidal gold techniques, was undertaken to further elucidate the nature and role of the *R. lignosus* EFS network during wood fragment degradation. Various cell surface markers, such as lectins, extensively used in the field of plant pathology (3, 12, 48) were tested for consistent characterization and visualization of sugar-containing molecules. Localization of RNA (4), β-1,3-glucans (13) and β-glucopyranosides (2) and wood cellulose degradation were also studied by means of enzyme-gold complexes (41). In parallel, immunogold labeling was performed on wood infected by *R. lignosus* for detection of (i) fimbriae, cell surface proteins of several fungi (5), (ii) pectin-containing molecules (31), and (iii) laccase of *R. lignosus*, a polyphenoloxidase involved in lignin degradation (22) as a powerful tool for better understanding the role of sheath fibrils in wood degradation (43).

MATERIALS AND METHODS

Fungal strains. *R. lignosus* 1 was isolated from infected rubber tree roots in the Ivory Coast. It was routinely maintained on 2.5% malt agar (Difco, Detroit, Mich.) plates. Laccase production and assay have been described elsewhere (23, 24).

Tissue processing. Wood slices (0.5 by 0.2 by 0.1 cm) were taken from fresh birch (*Betula papyrifera*), autoclaved for 1 h at 110°C, and placed at the edges of 2-day-old *R. lignosus* malt agar cultures. Autoclaved slices used as a control were placed on noninoculated malt agar cultures. All dishes were

* Corresponding author.

TABLE 1. Optimal conditions for formation of lectin-gold and enzyme-gold probes

Lectin or enzyme	Substrate specificity	pH of colloidal gold for conjugation
β-1,4-Exoglucanase	β-1,4-Glucans	9.0
β-Glucosidase	β-Glucosides	9.3
β-1,3-Glucanase	Laminarin	7.37
RNase	RNA	9.0
WGA	*N*-Acetylglucosamine	
Ovomucoid	WGA	4.95
Helix pomatia agglutinin	*N*-Acetylgalactosamine	7.4
Concanavalin A	α-D-Mannose, α-D-glucose	8.0
RcA	D-Galactose	8.0
Fetuin	LfA	5.4
LfA	Sialic acid	
Ulex europaeus agglutinin	α-D-Fucose	6.3

incubated in the dark at 28°C and approximately 90% relative humidity. At 3, 6, and 11 days later, sound and decayed wood slices were treated for transmission electron microscopy as previously described (1, 43, 44).

Cytochemistry. Polysaccharides were detected on thin sections by using the PATAg method (50, 52) modified as follows: periodic acid, 60 min; thiocarbohydrazide, 72 h; 1% silver proteinate, 30 min. Aniline blue (1/1,000 in distilled water) was used on living fungal cells for visualization of β-1,3-glucans. Observations were made on a Reichert Polyvar microscope with a Bp 450-490 exciter filter combined with a DS 510 and an LP 515 barrier filter for blue illumination.

Lectins and enzymes conjugated to colloidal gold were used as probes to localize different macromolecules in *R. lignosus* extracellular sheaths. Colloidal gold particles averaging 15 nm in diameter were prepared as described by Frens (20). The pH of the colloidal gold solution was adjusted in accordance with the isoelectric point of each enzyme and lectin used (Table 1). β-1,4-Glucans were localized by using an exoglucanase complexed to gold at pH 9 (41). RNase conjugated to gold at pH 9 (4) was used to localize RNA, and glucoside residues were localized with a β-glucosidase conjugated to gold at pH 9.3 (2). Localization of β-1,3-glucans was performed with β-1,3 glucanase purified from Zymolyase 20T (Seikagaku Corporation, Tokyo, Japan) and conjugated to colloidal gold at pH 7.37 (13). *N*-Acetylglucosamine, *N*-acetylgalactosamine, α-D-mannose and α-D-glucose, D-galactose, sialic acid, and α-L-fucose were localized by using, respectively, wheat germ agglutinin (WGA) followed by ovomucoid-gold at pH 4.95 (42), *Helix pomatia* agglutinin at pH 7.4 (48), concanavalin A at pH 8.0 (4), *Ricinus communis* agglutinin (RcA) at pH 8.0 (3), *Limax flavus* agglutinin (LfA) followed by fetuin-gold at pH 7.3 (49), and *Ulex europaeus* agglutinin at pH 6.3 (12).

The specificity of the different labelings was assessed by the following control tests: (i) incubation with gold-complexed protein to which was added the corresponding sugar molecule; β-1,4-glucans from barley for the exoglucanase-gold probe; RNA (Sigma) for the RNase probe; D-glucose for the glucosidase-gold probe; laminarin for the purified glucanase from Zymolyase 20T; *N*-acetylgalactosamine for the *H. pomatia* agglutinin-gold complex; D-mannose for the concanavalin A-gold complex, D-galactose for the RcA-gold complex, and α-L-fucose for the *Ulex europaeus* agglutinin-gold complex; (ii) incubation with WGA, previously adsorbed with *N*-acetyltrichitotriose, followed by incubation with the ovomucoid-gold complex; (iii) incubation with LfA, previously adsorbed with neuraminic acid (sialic acid), followed by incubation with the fetuin-gold complex.

Immunocytochemistry. Laccase purification, sodium dodecyl sulfate-native polyacrylamide gel electrophoretic patterns of the purified protein, and immunoblotting control of antibody specificity have been described previously (24, 43). For enzyme immunolocalization, ultrathin sections of nonosmicated infected wood chips were treated as described previously (43). Controls performed for immunolabeling of healthy and infected samples included (i) incubation with anti-laccase serum previously absorbed with the antigen, (ii) incubation with preimmune rabbit serum instead of the primary antiserum, and (iii) omission of the primary antibody incubation step.

Antiserum raised against fimbriae of *Ustilago violacea* was used to reveal the presence of fimbriae in *R. lignosus* sheaths. The procedure was similar to that described above for laccase localization, except that antibodies were used at a dilution of 1:50. Specificity of labeling was assessed as described previously (5).

Monoclonal antibodies (JIM5) raised against unesterified epitopes of pectin were used to visualize galacturonic acid-containing molecules over hyphal sheaths. Immunogold localization of pectin was performed as previously described by Knox et al. (31). Briefly, sections were incubated for 2 h at 37°C in a drop of primary antibodies and then for 30 min at 37°C on a drop of a gold-labeled goat anti-rat antibodies diluted 1:20. Specificity of labeling was assessed as described previously (31).

General controls. In addition to the controls described above, each gold probe was also used on other plant (tomato and pea) and fungal (*Ophiostoma ulmi*, *Fusarium* sp., and *Phellinus noxius*) embedded material on which these probes provide positive labeling.

Quantitation of labeling. To evaluate wood degradation after use of the exoglucanase-gold probe, the density of labeling over healthy and decayed wood was compared by determining the mean number of gold particles per square micrometer ± the standard error. Determinations of areas (*Sa*; two to three areas per micrograph) and numbers of gold particles (*Ns*) were made with Image, a picture-processing shareware, loaded on a Macintosh SE 30 computer (Apple). Density of labeling (*D*) was calculated as follows: $D = Ns/Sa$. For each estimation, 8 to 15 micrographs taken at magnifications of ×12,000 to ×40,000 were scanned.

RESULTS

Estimation of wood degradation by *R. lignosus*. The intensity of wood degradation by *R. lignosus* was evaluated by means of an exoglucanase-gold complex which specifically binds to free extremities of β-1,4-glucans of cellulose fibrils. Quantitation of gold particles revealed that density of labeling over infected wood cell walls decreased with inoculation times of 3, 6, and 11 days (557.35 ± 326.07, 259.45 ± 213.97, and 134.61 ± 51.12 gold particles per μm^2, respectively) after inoculation (d.a.i.) compared with the gold density of healthy wood (983.26 ± 71.44), the control (0.19 ± 0.1), and the background (0.87 ± 0.83). High standard error values at 3 and 6 days indicate a great variation in wood degradation.

Ultrastructure of *R. lignosus* extracellular sheaths during wood degradation. Examination of samples fixed with glutaraldehyde showed that EFS of *R. lignosus* was fibrillar in

appearance both close to and far from fungal cells (Fig. 1a). Only small granules were localized around hyphae in double-fixed material (Fig. 1b). The use of an exoglucanase-gold complex was helpful for distinction between EFS and wood cell walls (Fig. 1a), since *R. lignosus* hyphae were free of labeling (Table 2). Also, the positive PATAg staining reaction of EFS facilitated its visualization within the host since no staining was observed over wood cell walls (Fig. 1c). Sheaths were seldom seen surrounding hyphae at 3 d.a.i. of wood chips (Fig. 2a); they were commonly associated with hyphae at 6 d.a.i. (Fig. 2c) and were routinely observed at 11 d.a.i. (Fig. 3a to 4c). Despite this variation in frequency, in all cases sheaths were similar in appearance during wood fragment colonization. Although examinations of sections showed a variation in EFS thickness (Fig. 2a and b and 3a), sheaths always appeared fibrillar in nature, being dense adjacent to hyphal cell walls (Fig. 1a and c and 2d and e) and loose away from hyphae (Fig. 1a and 3a), where fibrils were distinctly observed. EFS was always closely associated with the fungal wall (Fig. 2b and e and 3b and c). Sheaths were rarely demarcated by a thin pellicle-like structure which could account for their outside smooth appearance (Fig. 4a and 5a).

Observations of wood colonization at 3 d.a.i. showed close contacts between *R. lignosus* sheaths and host cell walls without apparent wall degradation (Fig. 2c). Attack of xylem cells was associated with fungal fibrils that extended from hyphae into the host cell walls (Fig. 2d, e, and f). EFS could completely occupy the lumen of invaded xylem cells (Fig. 3a). These fibrils occurred at an appreciable distance from them (Fig. 1a and 3a), presumably preceding hyphal invasion. In both cases, the fibrils that filled the degraded areas (Fig. 2d) always appeared closely associated with eroded areas, as revealed by cytochemical tests (Fig. 3b to 4c). Advanced decay of wood was recognized by the lighter appearance of cell walls and a reduction in cellulose labeling (Fig. 4a). At this stage, wood cell wall fragments were often completely surrounded by EFS and fibrils were found to penetrate wood residues (Fig. 4a and b).

Cyto- and immunocytochemistry of *R. lignosus* EFS during wood degradation. Attempts to identify chemical components in *R. lignosus* EFS by means of enzymes or lectins conjugated to colloidal gold revealed labeling of sheaths only after treatment of wood sections with RcA for localization of galactose residues. In this case, few gold particles were observed over EFS (Table 2). Localization of chitin with the WGA–ovomucoid-gold complex succeeded only over fungal cell walls (Fig. 2b and e). Detection of glucopyranoside was performed with a β-glucosidase; sheaths did not exhibit any gold particles, while the fungal cytoplasm and cell wall displayed significant labeling (Table 2). β-1,3-Glucans were not detected by β-1,3-glucanase conjugated to colloidal gold, although weak fluorescence of the fungal cell wall was observed after staining with aniline blue (data not shown). Similarly, no labeling was observed over EFS after incubation of infected wood sections with an RNase-gold complex. A positive reaction for polysaccharide staining was recorded with the PATAg reaction (Table 2) over both the fungal cell wall and sheaths (Fig. 1c, 2a and f, and 4c). No staining of the xylem cell walls was noticed.

Immunolocalization of laccase produced by *R. lignosus* during wood degradation often revealed gold particles over the pellicle-bound (Fig. 5a) or wood cell-bordered (Fig. 5b) EFS. Sheaths associated with wood degradation displayed numerous gold particles. Labeling was also seen over both the *R. lignosus* cytoplasm and cell wall and altered wood cell wall layers (Fig. 5b). When labeling was observed over EFS, gold particles appeared to be closely associated with the fibrils (Fig. 5c). Control experiments showed no labeling when the primary antibody had been previously incubated with excess antigen or replaced with preimmune serum. Immunogold localization of fungal fimbriae following treatment with antibodies showed that gold particles were absent from EFS and restricted to fungal cell walls (Table 2). Fungal structures, including the extracellular material, did not exhibit any gold particles after treatment of sections with anti-pectin antibodies; weak labeling was observed over wood cell walls.

DISCUSSION

Cell surface interactions between plant cell walls and microorganisms have been widely studied, mainly with fungal (35, 54) and bacterial pathogens (33). Also, there is increasing evidence that extracellular material produced by fungi plays a key role in both plant pathogenesis and wood residue degradation. To gain new insights into the alteration of wood polymers by root-rotting fungi, we investigated an ultrastructural association between *R. lignosus* EFS and wood degradation in vitro.

Structure and possible origin of *R. lignosus* fibrillar sheaths. The fibrillar appearance of EFS was observed in samples fixed with glutaraldehyde but was absent in samples submitted to postfixation. In the latter samples, fine, dense precipitates possibly resulted from interactions between osmium tetroxide and prefixative residues or from a weak affinity of osmium for polysaccharides (28). In contrast, the appearance of sheaths produced by *Helminthosporium* sp. remained unchanged after the use of double fixation (55). The *R. lignosus* EFS had basically the same fibrillar structure independently of wood alteration levels and hyphal age, indicating that it was probably produced in the early stage of fungal growth in wood blocks. No particular EFS accumulation was observed at the apical regions of hyphae, as reported for *Phanerochaete chrysosporium* (51). Membrane elements were rarely seen, and no electron-dense inclusions were observed within *R. lignosus* sheaths, as pointed out for the white-rot fungus *Ganoderma* sp. (37), the scleroderris canker agent *Ascocalyx abietina* (4), or other brown-rot-causing organisms (19, 46, 47). Similarly, *R. lignosus* EFS was seldom limited by a denser bordering line such as that associated with brown-rot fungi (17, 46). Under our experimental conditions, electron micrographs always showed a fibrillar appearance of EFS both close to the fungal cell wall and at a considerable distance from hyphae. Bullock et al. (11) suggested that such EFS may originate from secretion of fibrillar material through the fungal wall. Some of our micrographs showed close connections between *R. lignosus* EFS and external portions of the fungal cell wall, indicating that the former could have formed apparently in continuity with the latter. Extracellular mycofibrils of *Postia placenta* have also been suggested to originate from the hyphal surface (32).

Chemical constitution of *R. lignosus* EFS. Work performed by Ruel and Joseleau (50) demonstrated the glucan nature of EFS differentiated by *P. chrysosporium*. Our cytochemical investigations revealed, however, that the nature of the polysaccharides present in the *R. lignosus* EFS and their spatial association with it may show noticeable differences from the EFS described by these and other workers. Although the PATAg reaction was strongly positive, the use of specific probes for characterization of chitin and β-1,3-

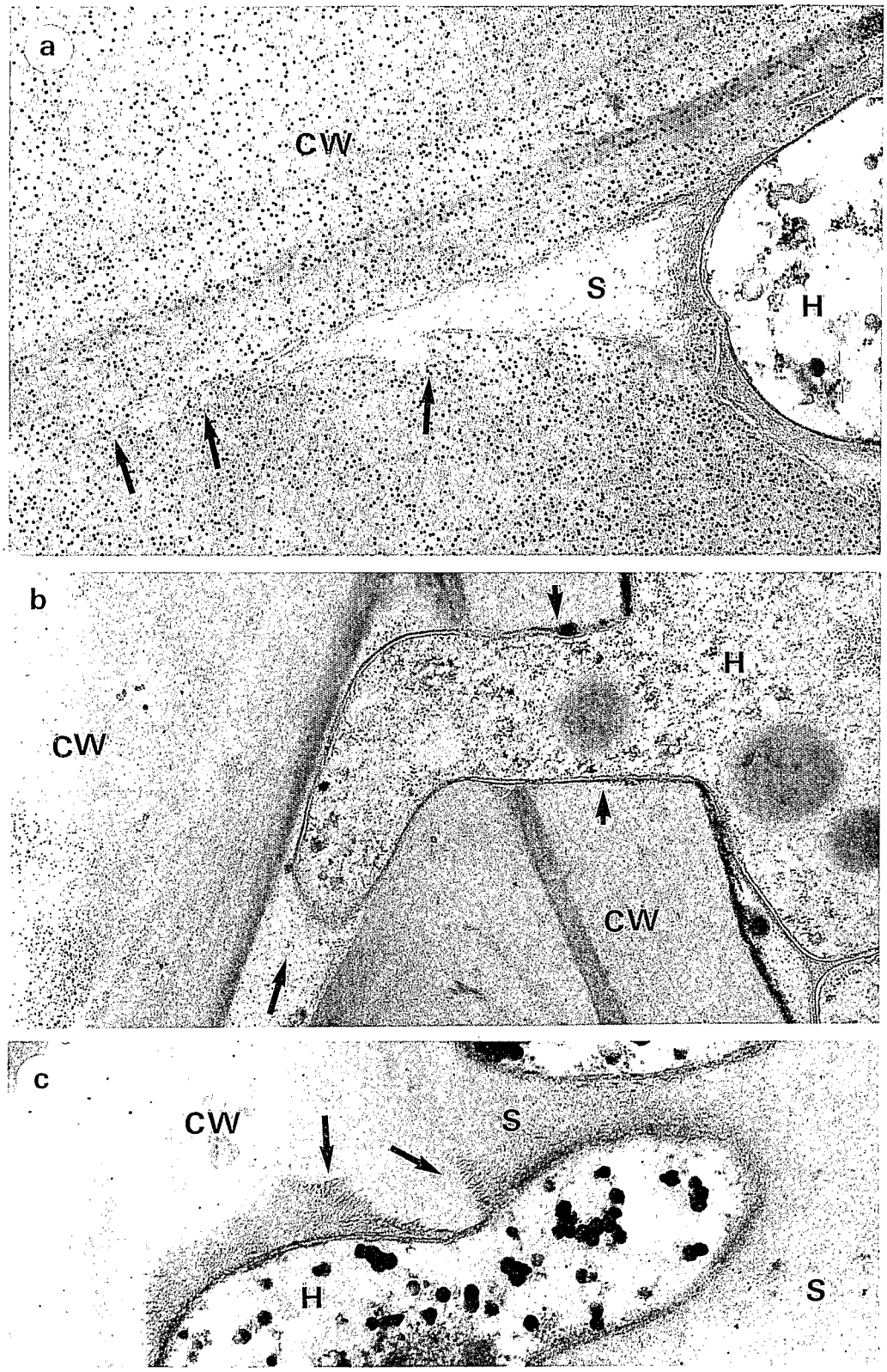

FIG. 1. Morphological appearance of *R. lignosus* EFS. (a) Infected wood fragments fixed with glutaraldehyde at 11 d.a.i. Labeling of cellulose with an exoglucanase conjugated to colloidal gold. Few or no gold particles are visible over the fungal sheath (S) and over the hypha (H). The EFS (S) is fibrillar in appearance both in close contact with the fungus and at a distance from it. Fibrils extend deeply into the wood cell walls (CW) some distance from the hypha; they are associated with cell wall degradation (arrows). Magnification, ×30,000. (b) Infected wood fragments fixed with glutaraldehyde and osmium tetroxide at 6 d.a.i. No fibrillar EFS is visible around the hypha; only small granules (arrows) are distributed near the mycelium. Note wood cell wall degradation (arrowheads) along the wall penetration channel. Hyphal cellular organelles are well preserved because of the double fixation. Magnification, ×22,500. (c) Infected wood fragments fixed with glutaraldehyde at 11 d.a.i. The section was treated with the PATAg test reagents for polysaccharides. This stain provides a positive reaction with the fungal sheath and cell wall, while the wood cell wall does not exhibit any labeling. A close association between EFS (S) and wall fragments (arrows) is apparent. Magnification, ×33,600.

TABLE 2. Semiquantitative results of cytochemical tests

Gold probe or staining	Substrate	Extent of labeling[a]			
		Wood cell wall	Mycelium		
			Sheath	Cell wall	Cytoplasm
Enzymes					
β-Glucosidase	β-Glucosides	0	0	1	3
β-1,4-Exoglucanase	β-1,4-Glucans	4	0	0	0
β-1,3-Glucanase	Laminarin	0	0	0	3
RNase	RNA	0	0	0	1–2
Lectins					
WGA + ovomucoid	*N*-Acetylglucosamine	3	0	2–3	0
Helix pomatia agglutinin	*N*-Acetylgalactosamine	0	0	0	1
Concanavalin A	α-D-Mannose, α-D-glucose	0	0	0	3
RcA	D-Galactose	0	0–1	2	1
LfA	Sialic acid	0	0	0	0
Ulex europaeus agglutinin	α-D-Fucose	0	0	1	0
Antibodies					
Anti-fimbriae (polyclonal)	Fimbriae	0–1	0	2	0
Anti-pectin (monoclonal)	Pectin	1	0	0	0
Anti-laccase (polyclonal)	Laccase	0–3	0–3	1–3	1–3
Other staining					
Aniline blue	β-1,3-Glucans	0	0	0–1	0
PATAg	Polysaccharides	0	3–4	3	2

[a] Rating scale: 0, no labeling; 1, weak labeling; 2, moderate labeling; 3, high labeling; 4, strong labeling.

glucans failed to demonstrate the presence of these compounds. This suggests that β-1,6-glucans, another group of ubiquitous fungal cell wall polysaccharides, could be among the main components of *R. lignosus* EFS, as they are for other fungi (10, 51). However, it is possible that β-1,3-glucans could be either highly substituted with β-1,6-linked glucans (51), thus preventing their accessibility to gold probes, or closely associated with proteins that inhibit binding sites. Similarly, the binding of glucans to fibrils of the sheath could also protect *N*-acetylglucosamine residues from binding to WGA.

The use of RcA indicated that galactose is a component of EFS and the cell wall. Minor sugars are known to play a role in the specificity of cell attachment and cell-cell recognition (34). In this respect, it may be expected that galactose-binding sites over fibrils of *R. lignosus* EFS are involved in such an interaction between the fungus and the plant surface. It has been reported that galactose residues of glycoproteins may display strong affinities for plant cell wall lectins (3). Although proteins that could have been involved in surface interactions (15, 26) were not detected in EFS, the binding sites for such proteins could nevertheless have also been masked. However, by using antibodies to fimbrial proteins, a positive reaction was found in cell walls of *R. lignosus*. Such fimbrial proteins were found to be abundant in EFS of *Stachybotrys elegans* during mycoparasitic interactions (6). Other polysaccharides, such as β-glucopyranosides, pectin, cellulose, mannose, *N*-acetylgalactosamine, sialic acid, and fucose, found in other fungi (27, 45, 50) were not detected in sheaths of *R. lignosus*.

The lack (or differences in the type) of labeling found with the cytochemical tests used, compared with other work with EFS, does not indicate imprecision of techniques, as such tests conducted concomitantly with other fungi gave positive results. Such apparent negative results are considered, rather, to disclose an interesting heterogeneity in either the composition or the structural arrangement of EFS of fungi.

Role and biological significance of *R. lignosus* fibrillar sheaths. In this work, the relationship between EFS and host cell wall breakdown was investigated by the use of labeled probes, thus providing more accurate pictures illustrating the involvement of the *R. lignosus* EFS in wood degradation. The EFS obviously was linked with plant cell wall alteration from initial wall penetration to late wood colonization over appreciable distances from hyphal cells, with sheath fibrils chiseling through host cell walls. In advanced decay, EFS fibrils or strands were closely associated with detached portions of host cell walls, even surrounding them. By filling degraded areas, fibrils of the EFS may maintain a moist environment favorable to fungal growth. It has been suggested that the presence of residual wood fragments within EFS likely provides a nutrient supply for the fungus, as reported for *Coriolus versicolor* sheaths (21). Accumulation of such nutrients may aid *R. lignosus* hyphae to survive in unfavorable environmental conditions, mainly in tropical areas where dry seasons are harmful for soil fungi and during which disease spread in plantations is stopped (39).

The occurrence of laccase in sheaths during wood colonization indicates that EFS carry wood-degradative proteins. Lignin peroxidases (8, 9, 51), xylanase (8, 26), and β-glucosidase (16, 21) are other enzymes involved in the breakdown of lignocelluloses that also have been localized within EFS of various wood-rotting fungi. Cytolocalization of these enzymes in EFS indicates that (i) degradation of wood polymers may occur within fungal sheaths and (ii) EFS provides translocation of wood-degrading enzymes from hyphal secreting sites toward releasing sites in host cell walls. However, uneven detection of laccase molecules in *R. lignosus* EFS suggests that localization of this enzyme in EFS may depend upon substrate accessibility. Interactions between glucan fibrils and lignocelluloses could represent an important step in the fungal attack of host cell walls (51). In this respect, one may speculate on mechanisms which control (i) recognition of wood substrates by fungal pathogens,

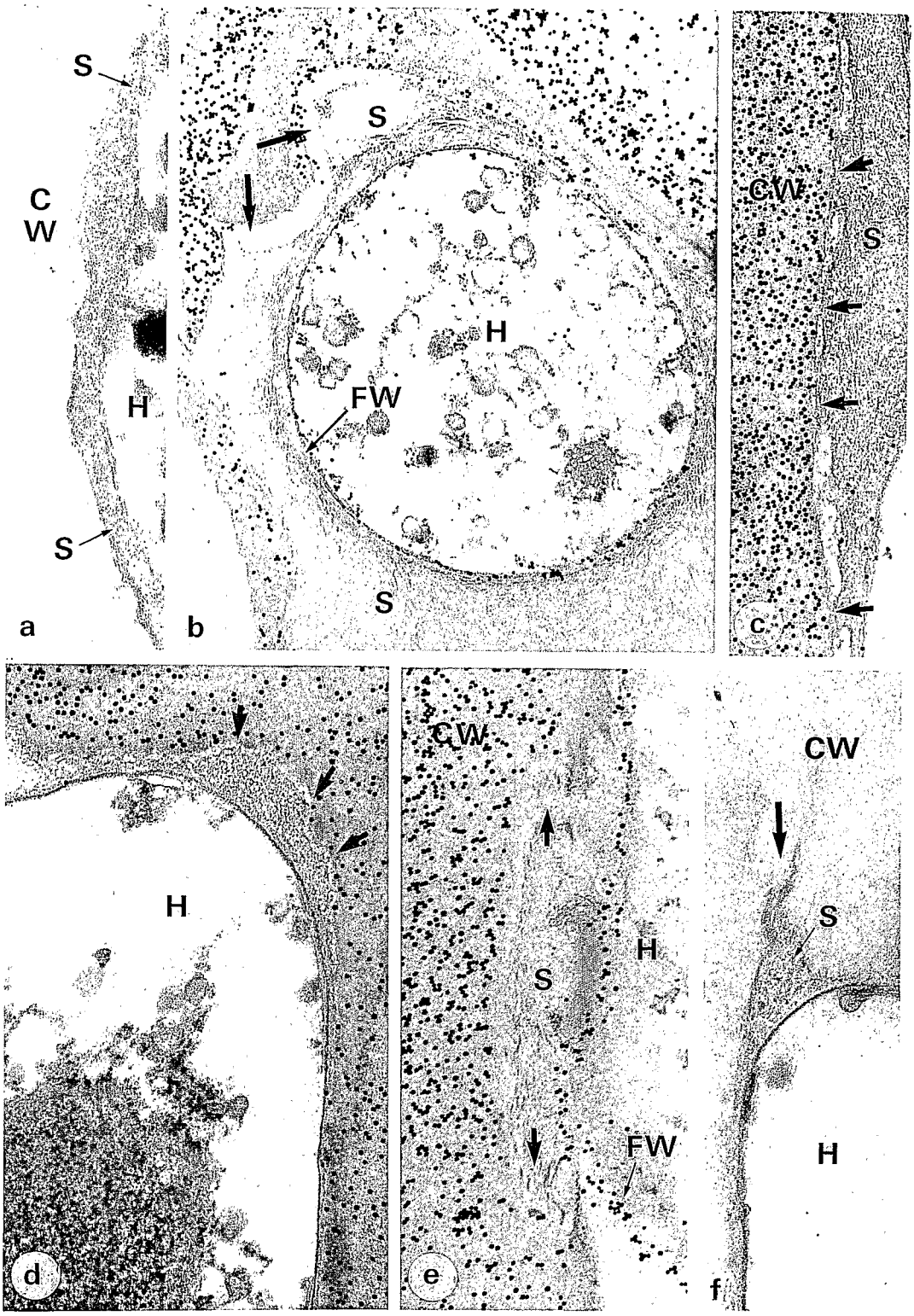

FIG. 2. Association of *R. lignosus* EFS with initiation of wood decay. (a) PATAg reaction for polysaccharides. The fungal sheath (S) completely surrounds the hypha (H) at 3 d.a.i. In contrast with the wood cell wall (CW), the EFS and the fungal cell wall show a positive PATAg reaction. EFS is closely associated with the fungal cell wall. Magnification, ×64,000. (b) Labeling of *N*-acetylglucosamine residues with WGA and an ovomucoid-gold complex. Labeling is apparent over the fungal cell wall (FW) and over the wood secondary walls, while no gold particles are visible over the EFS (S). A great variation in the sheath thickness is evident. The EFS is closely associated with both the fungal cell wall and host wall degradation at 11 d.a.i. (arrows). Magnification, ×28,000. (c) Labeling of cellulose with an exoglucanase-gold complex. The wood cell wall (CW) displays numerous gold particles; no significant labeling is evident over the fungal fibrillar sheath (S). Close contact (arrows) is visible between sheath fibrils and the apparently unaltered host cell wall at 6 d.a.i. Magnification, ×40,000. (d) Labeling of cellulose with an exoglucanase-gold complex. The degraded area of the wood cell wall (arrows) is filled by the unlabeled EFS at 6 d.a.i. Magnification, ×48,000. (e) Labeling of *N*-acetylglucosamine residues with WGA and an ovomucoid-gold complex. The unlabeled EFS (S) is closely associated with the fungal cell wall (CW), which exhibits gold particles. Fibrils of the fungal sheath extend from the fungal cell wall into the degraded wood cell wall (arrows) at 6 d.a.i. Magnification, ×40,000. (f) PATAg reaction for polysaccharides. Extension (arrow) of the EFS (S) within the host cell wall (CW) is associated with wood degradation at 6 d.a.i. Magnification, ×60,000.

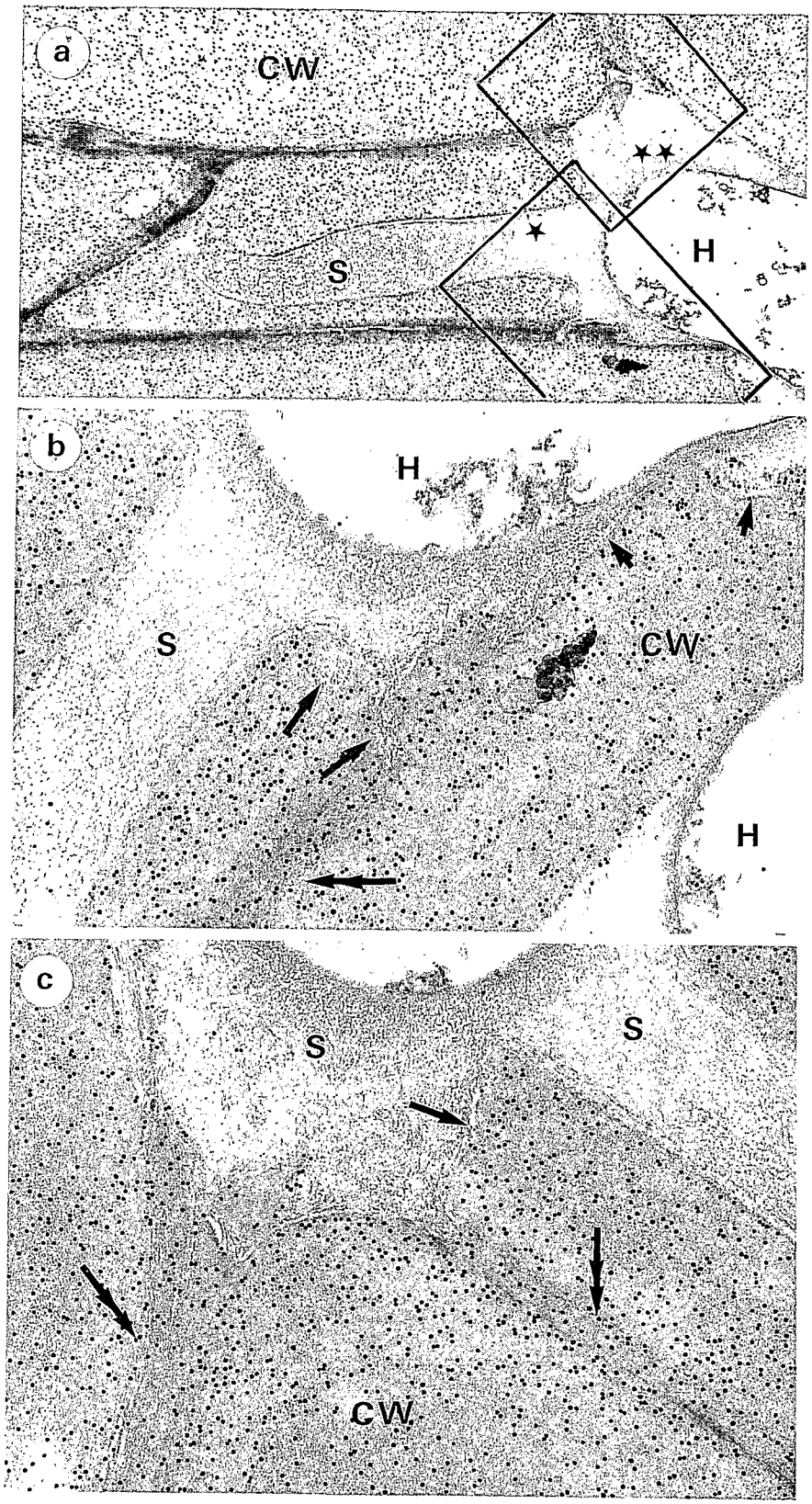

FIG. 3. Association of *R. lignosus* EFS with wood colonization at 11 d.a.i. Labeling of β-1,4-glucans with an exoglucanase-gold complex. (a) Fibrils of the unlabeled EFS (S) are compact close to the fungal wall (CW) and loose away from the hypha (H) at 11 d.a.i. The wood cell lumen is completely invaded by the fungal sheath (S). Magnification, ×15,000. (b and c) Enlargements of panel a insets * and **, respectively. Degradation of wood cell walls (CW) is associated with the EFS (S) both near the hypha (small arrows) and at a distance from it (large arrows). Fibrils also extend into slightly degraded wall areas (double arrows). Magnification, ×37,500.

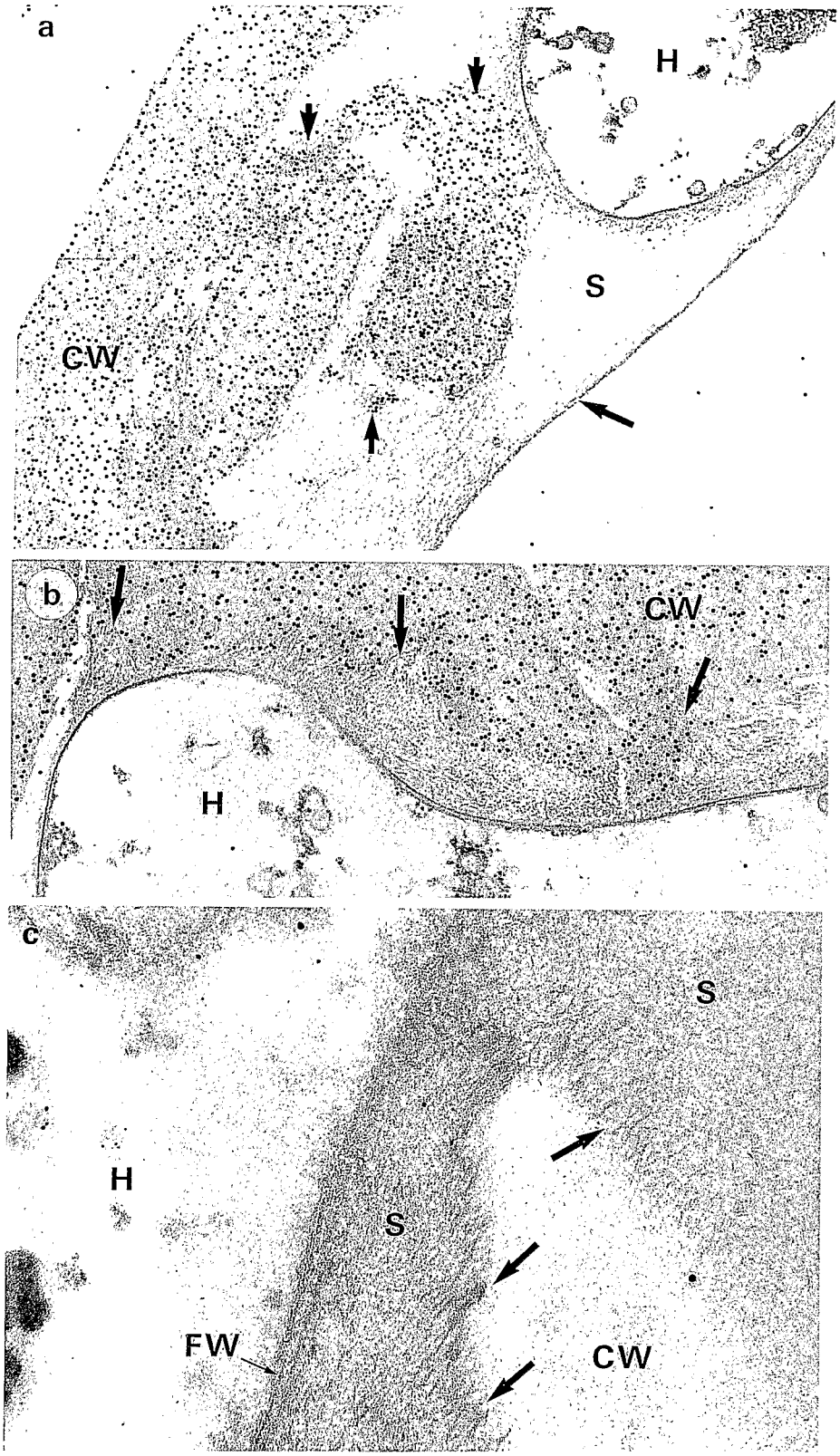

FIG. 4. Association of *R. lignosus* EFS with advanced wood decay at 11 d.a.i. (a) Labeling of cellulose with an exoglucanase-gold complex. Advanced decay is indicated by reduced labeling and more translucent areas of host cell walls (CW). Labeled wood fragments (small arrows) are enclosed within the fungal sheath (S). Fibrils surround and penetrate these wall portions. Notice the occurrence of a thin pellicle limiting the EFS (large arrow). H, hypha. Magnification, ×30,000. (b and c) Fibrils of *R. lignosus* EFS (S) are intimately associated (arrows) with degraded host cell walls (CW). They penetrate deeply into wood residues. (b) Labeling of cellulose with an exoglucanase conjugated to colloidal gold. Magnification, ×37,500. (c) PATAg reaction for polysaccharides. Magnification, ×81,000. FW, fungal cell wall.

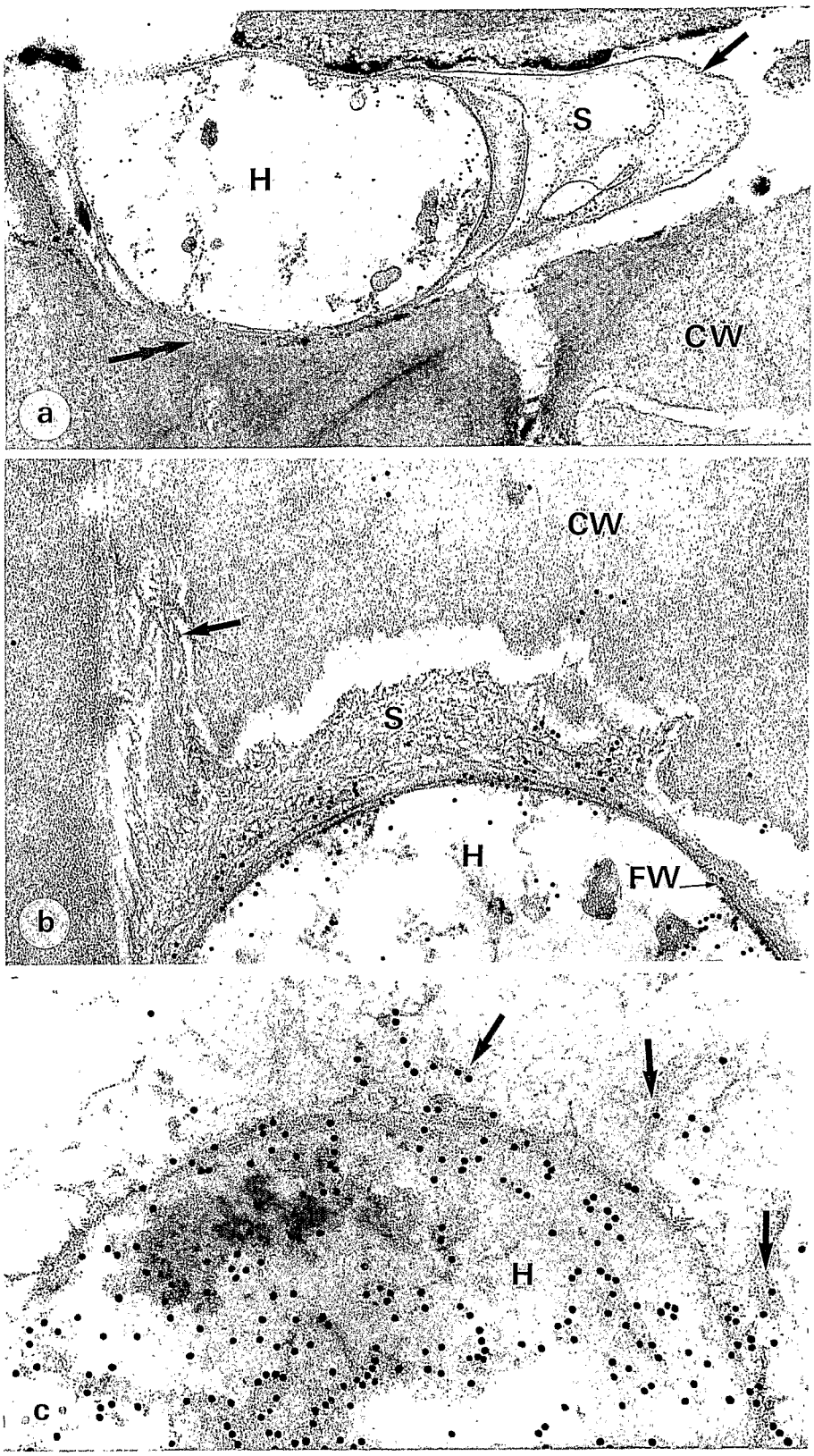

FIG. 5. Immunolocalization of *R. lignosus* laccase over EFS. (a) Laccase labeling is present over the EFS (S) and over the fungal cell wall and cytoplasm (H) at 11 d.a.i. Few gold particles are visible over wood cell walls. Note that a thin pellicle (arrow) surrounds the fungal sheath. Also, fibrils are associated with wood cell wall (CW) penetration (double arrow). Magnification, ×30,000. (b) Gold particles are present over *R. lignosus* EFS (S). Laccase is also localized over the fungal cell wall (FW) and the wood cell wall (CW). The fibrillar sheath fills degraded wall areas, extending deep into host cell walls (arrow) at 11 d.a.i. Magnification, ×56,000. (c) Numerous gold particles occur over the fungal cytoplasm (H). Similarly, laccase is visible over fibrils of the EFS (arrows) and over the fungal cell wall at 6 d.a.i. Magnification, ×80,000.

(ii) secretion of degrading enzymes from the fungal cytoplasm, (iii) transport of these enzymes by EFS, and (iv) their release in contact with, or close to, their specific substrates. Modifications, if any, in charge, size, and viscosity (i.e., hydrolysis of glucans) (51) might change EFS morphology and chemical composition, leading to control of fungal enzyme secretion. In addition, transport of wood-degrading enzymes by glucan fibrils toward their substrates would be consistent with findings that oxidases are not able to diffuse freely into intact wood (8, 43). Also, the inability of free oxidases to initiate lignocellulose breakdown (8, 16, 21, 51) may be explained by the presence in EFS of mediators that could be responsible for the initial attack of wood polymers. Accordingly, our electron micrographs showed a close association between *R. lignosus* EFS and early erosion of host cell walls.

R. lignosus is a well-known pathogen of numerous trees (23–25, 38). Previous ultrastructural findings (42, 44) have shown that fungal cells with EFS occurred in roots of infected rubber trees, raising the question of sheath function during pathogenesis. Compared with extracellular matrices produced by other fungal parasites, the constitution, structure, and role of EFS in wood decay fungi within living trees are poorly documented. In other plant diseases, it has been shown that matrices of *Colletotrichum* species (35, 36, 54) not only were involved in spore attachment but also contained enzymes that may function in plant penetration. Although we have no evidence of functions of the *R. lignosus* EFS in planta, it is likely that it determines the pathogen's ability to infect trees. In this respect, it seems that the interhyphal connecting material (rich in polysaccharides but poor in chitin) (42) within growing rhizomorphs of *R. lignosus* is the recognition structure that contributes to initiation of successful penetration of woody tissues by infective hyphae (41, 42, 44). As a great variation in virulence has been found among *R. lignosus* strains, it would be of interest to determine whether sheaths are required for tree infection. Moreover, EFS may also help hyphae to avoid plant defenses by constituting a selective barrier to fungitoxic molecules since *R. lignosus* laccases have been demonstrated to polymerize released phenols from lignin degradation (22).

In light of our results and other works, EFS of wood-degrading fungi may be important in both biodegradation of soil organic compounds and plant infection. If so, it may be suspected that fungal sheaths are involved in specific recognition mechanisms that activate genes that control pathogenicity factors. In addition, since a recent trend in research on plant disease resistance is to enrich these plants with hydrolases able to degrade fungal walls and such sheaths around fungal cells could well protect them against such hydrolytic enzymes, all due attention should be given to the occurrence and possible varietal composition of such sheaths in any plant disease system.

In summary, besides adding to the list of fungi that produce extracellular sheaths, our findings indicate that noticeable differences exist between these sheaths, not only in function, but also in structure and composition. The EFS features of *R. lignosus* are striking in that the EFS is composed of structures that extend freely in length for more than the diameter of the supporting cell. It would be very promising to isolate the genes responsible for this striking generating power with "transformers" likely in the sheath itself, as well as within the cell. Further knowledge of the various aspects of the mode of formation and action of such sheaths would lead to better insight not only into mechanisms of host cell wall attacks but also into the structural organization of host cell walls themselves.

ACKNOWLEDGMENTS

We thank A. Day and K. Roberts for kindly providing antibodies raised against fimbrial proteins and pectin, respectively, and C. Breuil for providing exoglucanase. We also thank M. Simard and C. Moffet for helpful technical assistance and K. Ruel and M. Lourd for reading the manuscript.

REFERENCES

1. **Abad, A. R., K. R. Cease, and R. A. Blanchette.** 1988. A rapid technique using epoxy resin Quetol 651 to prepare woody plant tissues for ultrastructural study. Can. J. Bot. **66:**677–682.
2. **Bendayan, M., and N. Benhamou.** 1987. Ultrastructural localization of glucoside residues on tissue sections by applying the enzyme-gold approach. J. Histochem. Cytochem. **35:**1149–1155.
3. **Benhamou, N., H. Chamberland, G. B. Ouellette, and F. Pauzé.** 1988. Detection of galactose in two fungi causing wilt diseases and their plant host tissues by means of gold-complexed *Ricinus communis* agglutinin. Physiol. Mol. Plant Pathol. **32:**249–266.
4. **Benhamou, N., and G. B. Ouellette.** 1987. Ultrastructural characterization of an extracellular sheath on cells of *Ascocalyx abietina*, the scleroderris canker agent of conifers. Can. J. Bot. **65:**154–167.
5. **Benhamou, N., G. B. Ouellette, R. B. Gardiner, and A. W. Day.** 1986. Immunocytochemical localization of antigen-binding sites in the cell surface of two ascomycete fungi using antibodies produced against fimbriae from *Ustilago violacea* and *Rhodotorula rubra*. Can. J. Bot. **32:**871–883.
6. **Benyagoub, M., H. Chamberland, and S. H. Jabaji-Hare.** 1992. Cytochemical study of the mycoparasitic interaction of *Stachybotrys elegans* with *Rhizoctonia solani*. Phytopathology **82:** 1119. (Abstract.)
7. **Blanchette, R. A.** 1991. Delignification by wood-decay fungi. Annu. Rev. Phytopathol. **29:**381–398.
8. **Blanchette, R. A., A. R. Abad, K. R. Cease, R. L. Farrell, R. E. Lovrien, and T. D. Leathers.** 1989. Enzyme immunocytochemistry and ultrastructural localization of cell wall components by enzyme-gold complexes, p. 69–81. *In* T. K. Kirk and H. M. Chang (ed.), Biotechnology in pulp and paper manufacture. Applications and fundamental investigations. Butterworth-Heineman, Boston.
9. **Blanchette, R. A., A. R. Abad, R. L. Farrell, and T. D. Leathers.** 1989. Detection of lignin peroxidase and xylanase by immunocytochemical labeling in wood decayed by basidiomycetes. Appl. Environ. Microbiol. **55:**1457–1465.
10. **Buchala, A. J., and M. Leisola.** 1987. Structure of the β-D-glucan secreted by *Phanerochaete chrysosporium* in continuous culture. Carbohydr. Res. **175:**146–149.
11. **Bullock, S., A. E. Ashford, and H. J. Willetts.** 1980. The structure and histochemistry of sclerotia of *Sclerotia minor* Jagger. II. Histochemistry of extracellular substances and cytoplasmic reserves. Protoplasma **104:**333–351.
12. **Chamberland, H., and J. G. Lafontaine.** 1992. Ultrastructural localization of L-fucose residues in nuclei of root primordia of the green pea *Pisum sativum*. Histochem. J. **24:**1–8.
13. **Chamberland, H., N. Lecours, M. Nicole, and G. B. Ouellette.** Unpublished data.
14. **Dowsett, J. A., and J. Reid.** 1981. Extracellular hyphal sheaths of *Dactylaria brochopaga*. Mycologia **73:**1207–1211.
15. **Epstein, L., L. B. Laccetti, and R. C. Staples.** 1987. Cell-substratum adhesive protein involved in surface contact responses of the bean rust fungus. Physiol. Mol. Plant Pathol. **30:**373–388.
16. **Evans, C. S., I. M. Gallagher, P. T. Atkey, and D. A. Wood.** 1991. Localization of degradative enzymes in white-rot decay of lignocellulose. Biodegradation **2:**93–106.
17. **Evans, R. C., and H. Stempen.** 1980. Evidence for pellicle-bound excrescences on hyphal walls of *Bipolaris maydis*. Mycologia **72:**523–533.

18. **Evans, R. C., H. Stempen, and S. J. Stewart.** 1981. Development of hyphal sheaths in *Bipolaris maydis* race T. Can. J. Bot. **59:**453–459.
19. **Foisner, R., K. Messner, H. Stachelberger, and M. Röhr.** 1985. Wood decay by basidiomycetes: extracellular tripartite membranous structures. Trans. Br. Mycol. Soc. **85:**257–266.
20. **Frens, G.** 1973. Controlled nucleation for regulation of the particle size in monodisperse gold suspensions. Nat. Phys. Sci. **241:**20–22.
21. **Gallagher, M. I., and C. S. Evans.** 1990. Immunogold-cytochemical labelling of β-glucosidase in the white-rot fungus *Coriolus versicolor*. Appl. Microbiol. Biotechnol. **32:**588–593.
22. **Geiger, J. P., B. Huguenin, M. Nicole, and D. Nandris.** 1986. Laccases of *Rigidoporus lignosus* and *Phellinus noxius*. II. Effect of *R. lignosus* laccase L1 on thioglycolic lignin of *Hevea*. Appl. Biochem. Biotechnol. **13:**97–110.
23. **Geiger, J. P., M. Nicole, D. Nandris, and B. Rio.** 1986. Root rot diseases of *Hevea brasiliensis*. I. Physiological and biochemical aspects of root aggression. Eur. J. For. Pathol. **16:**22–36.
24. **Geiger, J. P., B. Rio, D. Nandris, and M. Nicole.** 1986. Laccases of *Rigidoporus lignosus* and *Phellinus noxius*. I. Purification and some physico-chemical properties. Appl. Biochem. Biotechnol. **12:**121–133.
25. **Geiger, J. P., B. Rio, M. Nicole, and D. Nandris.** 1986. Biodegradation of *Hevea brasiliensis* wood by *Rigidoporus lignosus* and *Phellinus noxius*. Eur. J. For. Pathol. **16:**147–159.
26. **Green, F., III, C. A. Clausen, M. J. Larsen, and T. L. Highley.** 1992. Immuno-scanning electron microscopic localization of extracellular wood-degrading enzymes within the fibrillar sheath of the brown-rot fungus *Postia placenta*. Can. J. Microbiol. **38:**898–904.
27. **Harder, D. E., J. Chong, R. Rohringer, K. Mendgen, A. Schneider, K. Welter, and G. Knauf.** 1988. Ultrastructure and cytochemistry of extramural substances associated with intercellular hyphae of several rust fungi. Can. J. Bot. **67:**2043–2051.
28. **Hayat, M. A.** 1981. Principles and techniques of electron microscopy. Biological application, vol. 1, 2nd ed., p. 13–89. University Park Press, Baltimore.
29. **Highley, T. L., J. G. Palmer, and L. L. Murmanis.** 1983. Decomposition of cellulose by *Poria placenta*: light and electron microscopy study. Holzforschung **37:**179–184.
30. **Kim, Y. S., B. Goodell, and J. Jellison.** 1991. Immuno-electron microscopic localization of extracellular metabolites in spruce wood decayed by brown-rot fungus. Holzforschung **45:**389–393.
31. **Knox, J. P., P. J. Linstead, J. King, C. Cooper, and K. Roberts.** 1990. Pectin esterification is spatially regulated both within cell walls and between developing tissues of root apices. Planta (Heidelberg) **181:**512–521.
32. **Larsen, M. J., and F. Green III.** 1992. Mycofibrillar cell wall extensions in the hyphal sheath of *Postia placenta*. Can. J. Microbiol. **38:**905–911.
33. **Leigh, J. A., and D. L. Coplin.** 1992. Exopolysaccharides in plant-bacterial interactions. Annu. Rev. Microbiol. **46:**307–346.
34. **Manocha, M. S., and Y. Chen.** 1990. Specificity of attachment of fungal parasites to their hosts. Can. J. Microbiol. **36:**69–76.
35. **McRae, C. F., and G. R. Stevens.** 1990. Role of conidial matrix of *Colletotrichum orbiculare* in pathogenesis of *Xanthium spinosum*. Mycol. Res. **94:**890–896.
36. **Mondal, A. H., and D. G. Parbery.** 1992. The spore matrix and germination in *Colletotrichum musae*. Mycol. Res. **96:**592–596.
37. **Murmanis, L., T. L. Highley, and J. G. Palmer.** 1984. An electron microscopy study of western hemlock degradation by the white-rot fungus *Ganoderma applanatum*. Holzforschung **38:**11–18.
38. **Nandris, D., M. Nicole, and J. P. Geiger.** 1987. Root rot diseases of rubber-tree. Plant Dis. **71:**298–306.
39. **Nandris, D., M. Nicole, and J. P. Geiger.** 1988. Root rot diseases of rubber tree. I. Severity, dynamics and characterization of epidemics. Can. J. For. Res. **18:**1248–1254.
40. **Nicholson, R. L., J. Hipskind, and M. Hanau.** 1989. Protection against phenol toxicity by the spore mucilage of *Colletotrichum graminicola*, an aid to secondary spread. Physiol. Mol. Plant Pathol. **35:**243–252.
41. **Nicole, M., and N. Benhamou.** 1991. Cytochemical aspects of cellulose breakdown during the infection process of rubber tree roots infected by *Rigidoporus lignosus*. Phytopathology **81:**1412–1420.
42. **Nicole, M., and N. Benhamou.** 1991. Ultrastructural localization of chitin in cell walls of *Rigidoporus lignosus*, the white-rot root fungus of rubber trees. Physiol. Mol. Plant Pathol. **39:**415–432.
43. **Nicole, M., H. Chamberland, J. P. Geiger, N. Lecours, J. Valéro, B. Rio, and G. B. Ouellette.** 1992. Immunocytochemical localization of laccase L1 in wood decayed by *Rigidoporus lignosus*. Appl. Environ. Microbiol. **58:**1727–1739.
44. **Nicole, M., J. P. Geiger, and D. Nandris.** 1987. Ultrastructural aspects of rubber tree root rot diseases. Eur. J. For. Pathol. **17:**1–10.
45. **Nicole, M., K. Ruel, and G. B. Ouellette.** Fine morphology of fungal structures involved in host cell wall alterations. *In* O. Petrini and G. B. Ouellette (ed.), Host wall alteration by parasitic fungi, in press. APS Press, St. Paul, Minn.
46. **Palmer, J. G., L. Murmanis, and T. L. Highley.** 1983. Visualization of hyphal sheath in wood decay Hymenomycetes. I. Brown-rotters. Mycologia **75:**995–1004.
47. **Palmer, J. G., L. Murmanis, and T. L. Highley.** 1983. Visualization of hyphal sheath in wood decay Hymenomycetes. II. White-rotters. Mycologia **75:**1005–1009.
48. **Roth, J.** 1983. Application of lectin-gold complexes for electron microscopic localization of glycoconjugates on thin sections. J. Histochem. Cytochem. **31:**987–997.
49. **Roth, J., J. M. Lucocq, and P. M. Charest.** 1984. Light and electron microscopic demonstration of sialic acid residues with the lectin from *Limax flavus*: a cytochemical affinity technique with the use of fetuin-gold complexes. J. Histochem. Cytochem. **32:**1167–1176.
50. **Ruel, K., and J.-P. Joseleau.** 1991. Involvement of an extracellular glucan sheath during degradation of *Populus* wood by *Phanerochaete chrysosporium*. Appl. Environ. Microbiol. **57:**374–384.
51. **Ruel, K., E. Odier, and J.-P. Joseleau.** 1989. Immunocytochemical observations of fungal enzymes during degradation of wood cells by *Phanerochaete chrysosporium* (strain K-3), p. 83–97. *In* T. K. Kirk and H. M. Chang (ed.), Biotechnology in pulp and paper manufacture. Applications and fundamental investigations. Butterworth-Heineman, Boston.
52. **Thiery, J. P.** 1967. Mise en évidence des polysaccharides sur coupes fines en microscopie électronique. J. Microsc. (Paris) **6:**987–1018.
53. **Tsuneda, A., N. Maekawa, I. Ohara, and I. Furukawa.** 1991. Incipient decay of *Quercus serrata* sapwood by *Lentinus edodes* and its inhibition by an antagonistic hyphomycete, *Leptodontidium elatius*. Can. J. Bot. **69:**2792–2805.
54. **Van Dyke, C. G., and C. M. Mims.** 1991. Ultrastructure of conidia, conidium germination, and appressorium development in the plant pathogenic fungus *Colletotrichum truncatum*. Can. J. Bot. **69:**2455–2467.
55. **Wheeler, H., and D. Gantz.** 1979. Extracellular sheaths on hyphae of two species of *Helminthosporium*. Mycologia **71:**1127–1135.